ЖЭТФ, 2013, том 144, вып. 6 (12), стр. 1153–1164

ESTIMATE OF THE FRACTION OF PRIMARY PHOTONS IN THE COSMIC-RAY FLUX AT ENERGIES $\sim 10^{17}$ eV FROM THE EAS-MSU EXPERIMENT DATA

Yu. A. Fomin [a], ***N. N. Kalmykov*** [a]*, ***G. V. Kulikov*** [a], ***V. P. Sulakov*** [a], ***S. V. Troitsky*** [b]**

[a] *Skobeltsyn Institute of Nuclear Physics, Lomonosov Moscow State University 119991, Moscow, Russia*

[b] *Institute for Nuclear Research, Russian Academy of Sciences 117312, Moscow, Russia*

Received May 27, 2013

We reanalyze archival EAS-MSU data in order to search for events with an anomalously low content of muons with energies $E_\mu > 10$ GeV in extensive air showers with the number of particles $N_e \gtrsim 2 \cdot 10^7$. We confirm the first evidence for a nonzero flux of primary cosmic gamma rays at energies $E \sim 10^{17}$ eV. The estimated fraction of primary gamma rays in the flux of cosmic particles with energies $E \gtrsim 5.4 \cdot 10^{16}$ eV is $\epsilon_\gamma = \left(0.43^{+0.12}_{-0.11}\right)$ %, which corresponds to the intensity $I_\gamma = \left(1.2^{+0.4}_{-0.3}\right) \cdot 10^{-16}$ cm$^{-2} \cdot$ s$^{-1} \cdot$ sr^{-1}. The study of arrival directions does not favor any particular mechanism of the origin of the photon-like events.

DOI: 10.7868/S0044451013120043

1. INTRODUCTION

The study of the primary mass composition of ultra-high-energy (UHE) cosmic rays (CR) is one of the topical problems of astroparticle physics because these experimental results are of crucial importance for understanding the theory of both cosmic-ray generation in their sources and their subsequent propagation to Earth. The low UHECR intensity makes their study by direct methods impossible, and hence the only available method is the study of extensive air showers (EASs).

The dominant part of EASs is caused by primary nuclei (from protons to iron), but there is a considerable interest in the possible presence of very different particles, e. g., UHE gamma rays, among them. First works on the subject already appeared half a century ago (see, e. g., Ref. [1]), but definitive quantitative results are still lacking (cf. review [2] and the references therein). Indeed, the highest-energy cosmic photons firmly detected had the energy of ~ 50 TeV [3]. The searches for gamma rays in the energy ranges $3 \cdot 10^{14}$ eV$\lesssim E \lesssim 5 \cdot 10^{16}$ eV (the EAS-TOP [4], CASA-MIA [5], and KASCADE [6] experiments) as well as at $E \gtrsim 10^{18}$ eV (the Haverah Park [7], AGASA [8–10], Yakutsk [11, 12], Pierre Auger [13, 14], and Telescope Array [15] experiments) did not find any signal and resulted in upper limits on the photon flux only. A few claims of the experimental detection of 10^{14} eV$\lesssim E \lesssim 10^{17}$ eV photons (Mt. Chacaltaya [16], Tien Shan [17], Yakutsk [18], and Lodz [19]) had low statistical significance. At the same time, a certain flux of UHE photons is predicted in many models of both the conventional and "new" physics. In particular, the flux of secondary photons from interactions of extreme-energy particles with cosmic background radiation, the so-called Greizen–Zatsepin–Kuzmin (GZK) photons, may serve as a tool to distinguish various models of cosmic rays at energies $\gtrsim 5 \cdot 10^{19}$ eV because the photon flux is very sensitive to the primary composition at these energies: a predominantly light composition at GZK energies results in a much higher flux of secondary photons. Given the present contradictory situation with the mass composition at UHE (see, e. g., Ref. [20] for a detailed review and Ref. [21] for a brief update), searches for GZK photons are now considered very important. Also, a significant contribution to the UHE gamma-ray flux is predicted in particular top-down mechanisms of the CR origin ([22] and the references therein), in particle physics models with Lorentz invariance violation [23], and in models with axion–photon mixing [24].

*E-mail: kalm@eas.sinp.msu.ru
**E-mail: sergey.troitsky@gmail.com

One of the most promising approaches to the search of primary gamma-rays is the study of the EAS muon component. The number of muons in a gamma-ray-induced EAS is an order of magnitude smaller than in a usual hadronic shower. Therefore, one may hope to find photon showers by selecting those that have an unusually low muon content.

In this paper, we study the muon content of showers with the estimated number of particles $N_e > 2 \cdot 10^7$ and zenith angles $\theta < 30^\circ$ detected by the EAS-MSU array [25] in 1982–1990. We demonstrate that the number of muonless events significantly exceeds the background expected from random fluctuations in the development of showers caused by primary hadrons. This result can be interpreted as an indication of the presence of gamma rays in the primary cosmic radiation with energies of the order of 10^{17} eV, which confirms and strengthens the first evidence for UHE cosmic photons [26].

The rest of the paper is organized as follows. In Sec. 2, we briefly review the experimental setup (Sec. 2.1), then discuss the data set we study, and muonless events in particular (Sec. 2.2). Section 3 is devoted to the estimate of the number of background muonless events for hadronic showers (Sec. 3.1) and to the derivation of the estimated photon flux under the assumption that all muonless events not accounted for by the hadronic background are caused by primary gamma rays (Sec. 3.2). Possible systematic errors in the determination of the flux are discussed in Sec. 3.3. In Sec. 4, we present a detailed study of the distribution of the arrival directions of muonless events on the celestial sphere and test various models of the origin of primary photons. We put our results in the context of the present-day state of the art and briefly conclude in Sec. 5.

2. EXPERIMENT AND DATA

2.1. The EAS-MSU array

The description of the EAS-MSU array is given in [25]. The array had the area of 0.5 km^2 and contained 77 charged-particle density detectors (consisting of Geiger–Müller counters) for determination of the EAS size N_e using an empirical lateral distribution function [27] and 30 scintillaion detectors that measured particle arrival times necessary for determination of the EAS arrival direction. In addition to the surface detectors that mostly recorded the electron–photon component of an EAS, the array also included four underground muon detectors, also consisting of

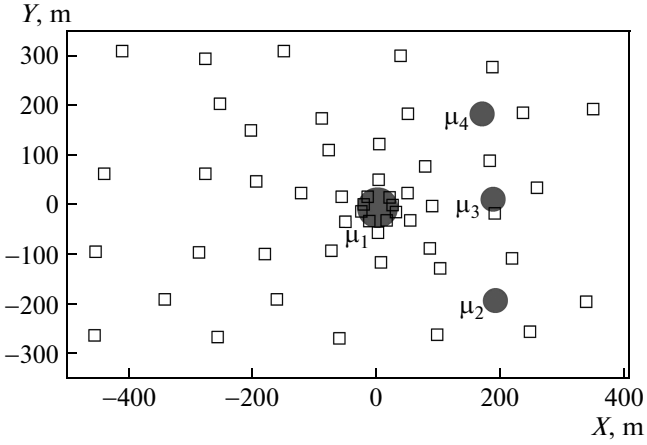

Fig. 1. The EAS-MSU array setup. Muon detectors (circles) are denoted by μ_i, $i = 1, \ldots, 4$; surface detector stations are represented by squares

Geiger–Müller counters, located at the depth of 40 meters of water equivalent. These detectors recorded muons with energies above 10 GeV. A muon detector with the area of 36.4 m^2 was located at the center of the array while the other three stations had the area of 18.2 m^2 and were located at the distances between 150 m and 300 m from the center (see Fig. 1). To select the sample of showers with the number of particles $N_e > 2 \cdot 10^7$ that we use in this work, 22 scintillaion detectors, each of the area of 0.5 m^2, were used. The scintillaion detector threshold was set at the level of 1/3 of a relativistic particle. The temporal resolution was ~ 5 ns. The 22 stations formed 13 systems of 4-fold coincidences between counters located at the vertices of tetragons with sides between 150 m and 300 m, which allowed efficiently selecting the showers on the full array area. The scintillaion detectors were located at the same points as the Geiger–Müller counters. The master criterion was determined by the firing, in the time gate of ~ 6 μs, of at least one of the 4-fold coincidence systems.

With these selection criteria implemented, the probability of detection of a shower with $N_e > 2 \cdot 10^7$ falling to any place of the array was not less than 95 %. The position of the shower axis was determined with the precision of $\sim$ 10 m. The precision of determining the arrival direction was $\sim 3^\circ$. The number of particles in the shower was determined with the accuracy $\sim$ (15–20) %.

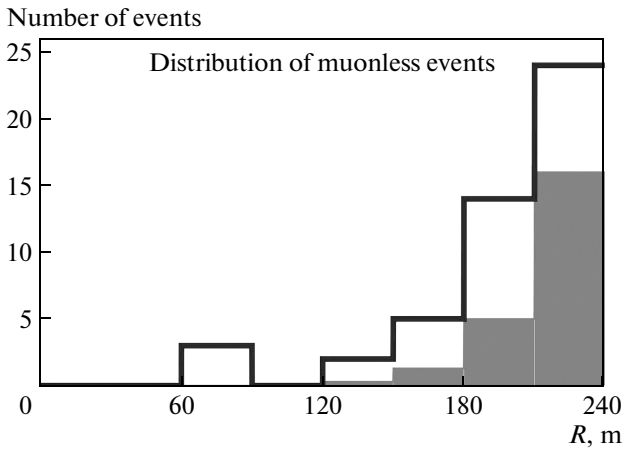

Fig. 2. The distribution of muonless events over the distance R between the shower axis and the muon detector. Line: data; shadow: expectation for hadronic primaries

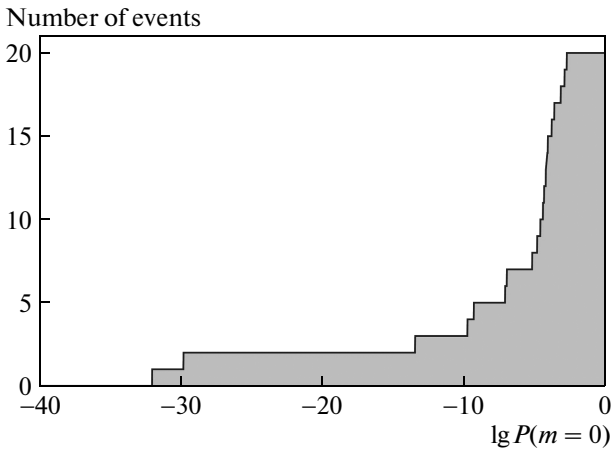

Fig. 3. Cumulative distribution of muonless events in the LDF-based Poisson probability $P(m = 0)$

2.2. The data set and muonless events

The presence of muon detectors in the EAS-MSU array allows searching for primary gamma rays. The method is based on the fact that for $N_e \gtrsim 10^7$ and for an hadronic primary, it is highly unprobable to have zero muons in the central, 36.4 m^2, detector if the shower axis is within ~ 240 m from it. At the same time, these muonless events are fully consistent with the conjecture of primary gamma rays. The total number of events with $N_e \geq 2 \cdot 10^7$ in the data set is 1679; 48 of them are muonless.

Figure 2 presents the distribution of muonless events over the distance R between the shower axis and the muon detector. Most of the muonless events correspond naturally to large R; however, there are a certain number of events close to the axis, which are very difficult to explain by random fluctuations of the hadronic background. We note that the real number of muonless events is larger than the observed one because of the non-EAS background that results in firing of each counter in the central muon detector with the average frequency of 4.6 Hz. In three other muon detectors, the frequency of random firing was 2 to 3 times higher, and in this work, we use only the data of the central detector. It consisted of 1104 counters. For the time of EAS detection ~ 15 μs, we expect 0.076 random firings. Therefore, we assume that the probability of the absence of random firing was 0.93.

To obtain a very rough estimate of the probability to have a muonless hadronic event, we can start with the (experimentally known) mean muon lateral distribution function [27] and estimate the expected muon density $\rho_\mu(N_e, R)$ for a given core distance R. Then, using the Poisson distribution, we can calculate the probability $P(m = 0)$ to have no muons in the detector at this distance. In Fig. 3, the distribution of $m = 0$ events in $P(m = 0)$ is shown. The tail at low $P(m = 0)$ indicates that there might be a problem in explaining the observed number of muonless events within the standard model of the shower development.

3. ESTIMATES OF THE GAMMA-RAY FLUX

To quantify the observed discrepancy more precisely, we performed Monte Carlo simulations of proton-induced showers and compared the number of muonless events in data and in simulations.

3.1. Modeling artificial showers

For the shower simulations, we used the AIRES v. 2.6.0 [28] simulation code, whose choice was determined primarily by its speed. We used the high-energy hadronic interaction model QGSJET-01 [29]. The primary protons were thrown with zenith angles $0^\circ \leq \theta \leq 30^\circ$ and with energies between $3 \cdot 10^{16}$ eV and $2 \cdot 10^{17}$ eV, assuming the integral spectral index 2.0. Without the account of fluctuations, the energy of an $N_e = 2 \cdot 10^7$ proton shower would be equal to $E \sim 10^{17}$ eV; however, the fluctuations reduce this value. For the study, showers with $N_e \geq 2 \cdot 10^7$ have been selected; Fig. 4 gives the distribution of the primary energies of the selected artificial showers. In this

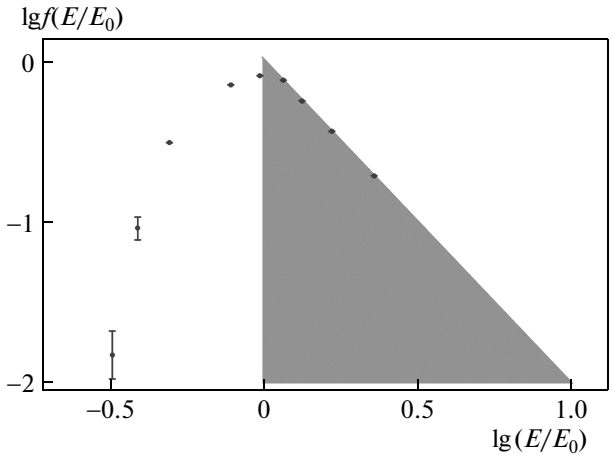

Fig. 4. Contribution of various primary energies to the proton showers with $N_e \geq 2 \cdot 10^7$. Points: results of the simulation; shadow: naive estimate without the account of fluctuations. $E_0 \approx 10^{17}$ eV

way, the total number of 15000 artificial showers was simulated.

3.2. Estimate of the fraction and flux of gamma rays

The general assumption behind our estimate of the gamma-ray flux is that all muonless events, not accounted for by fluctuations of hadronic showers, are caused by primary gamma rays. Therefore, the central point of the estimate is the calculation of the expected number of background muonless events from the simulated proton-induced showers.

The probability of a zero muon detector reading, $m = 0$, was estimated under the assumption (see Ref. [30] for its motivation) that muon density fluctuations in EAS can be represented as a superposition of (a) fluctuations of the muon density at a given distance from the shower axis, determined purely by the EAS development, and (b) the Poisson fluctuations of the number of particles that hit the detector station. In this approach, the probability $P(\Delta R, S, m)$ to have m muons in the detector of area S located in the annulus ΔR (at a distance between R and $R + \Delta R$ from the shower axis) is given by

$$P(\Delta R, S, m) = \int P_{\mathrm{EAS}}(\Delta R, M) P_{\mathrm{P}}(M, S, m)\, dM,$$

where $P_{\mathrm{EAS}}(\Delta R, M)$ is the function of the muon number density distribution in the annulus determined by the shower development and $P_{\mathrm{P}}(M, S, m)$ is the Poisson probability to record exactly m muons in a detector of the area S for the total number M of muons in the annulus.

We suppose that a shower axis came within the annulus

$$\Delta R_k = R_{k+1} - R_k$$

from the muon detector. Then the muon density in the annulus is determined as

$$\rho_\mu(\Delta R_k, i) = \frac{N_\mu(\Delta R_k, i)}{\pi\left(R_{k+1}^2 - R_k^2\right)},$$

where $N_\mu(\Delta R_k, i)$ is the number of muons in this annulus and $i = 1, \ldots, n_{tot}$ is the number of selected artificial showers. Then the probability of a zero detector reading in the ΔR_k annulus is

$$P(m = 0, \Delta R_k) = \\ = \frac{1}{n_{tot}} \sum_i^{n_{tot}} 0.93 \exp\left(-S \cos\theta \rho_\mu(\Delta R_k, i)\right),$$

where θ is the zenith angle of the shower.

The total probability of an $m = 0$ event is

$$P_{tot}(m = 0) = \sum_{k=1}^{k_{max}} P(m = 0, \Delta R_k) \frac{R_{k+1}^2 - R_k^2}{R_{k_{max}}^2},$$

where k_{max} gives the total number of annuli considered and the last factor accounts for the probability that the shower axis hits the ΔR_k annulus. The results of calculating the probability to observe a muonless event are given, for various distances from the shower axis, in Table 1 together with the number of observed and predicted muonless events in our sample of 1679 showers.

The total probability to have a muonless proton-induced event within 240 m between the detector and the shower axis is $1.4 \cdot 10^{-2}$, which corresponds to ≈ 23 expected muonless events in the sample, to be compared with 48 observed. As expected, the dominant part of the background muonless events should appear in two outer annuli we considered, the same being true also for the observed events. However, the total number of the observed events is almost twice the expected one. Based on the Poisson distribution, this allows estimating the number S of signal photon-like events in the sample as $S = 25.2^{+7.2}_{-6.6}$, which transforms into the fraction $\epsilon_1 = \left(1.50^{+0.43}_{-0.39}\right)$ % of anomalous muonless events in the sample with $N_e \geq 2 \cdot 10^7$ and $\theta \leq 30^\circ$.

We want to identify the anomalous muonless showers with showers initiated by primary photons. To determine the fraction of these events in the energy spectrum of cosmic rays, we need to take the difference in

Table 1. Observed and expected numbers of muonless events for various distances between the detector and the shower axis. See text for the notation

ΔR, m	Observed number of muonless events	$P(m=0,\Delta R)$	Expected number of muonless events
60–90	3	$1.8\cdot10^{-7}$	$3\cdot10^{-4}$
90–120	0	$7.7\cdot10^{-6}$	0.013
120–150	2	$2.15\cdot10^{-4}$	0.36
150–180	5	$8.0\cdot10^{-4}$	1.3
180–210	14	$3.2\cdot10^{-3}$	5.4
210–240	24	$9.8\cdot10^{-3}$	16.4
0–240	48	$1.4\cdot10^{-2}$	23.5

the development of showers caused by photons and protons of the same energy into account. The gamma-ray showers develop slower in the atmosphere and arrive younger to the surface level (the vertical atmospheric depth for EAS-MSU is 1025 g·cm^{-2}). On average, for the primary energies $\sim 10^{17}$ eV, the number of particles in a gamma-ray shower detected by the EAS-MSU experiment should be ≈ 1.86 times larger than in a proton shower. The cut in N_e we use thus corresponds, on average, to the gamma-ray energy $5.4\cdot10^{16}$ eV. Knowing the total cosmic-ray flux measured by the EAS-MSU array [31], we determine the main result in the present work: the photon fraction

$$\epsilon_\gamma = \left(0.43^{+0.12}_{-0.11}\right)\ \% \quad \text{for } E \gtrsim 5.4\cdot10^{16}\ \text{eV}$$

and the photon flux intensity

$$I_\gamma = \left(1.2^{+0.4}_{-0.3}\right)\cdot10^{-16}\ \text{cm}^{-2}\cdot\text{s}^{-1}\cdot\text{sr}^{-1} \quad \text{for } E \gtrsim 5.4\cdot10^{16}\ \text{eV}. \quad (1)$$

3.3. Estimate of systematic uncertainties

The systematic uncertainty of our result, within the method we use, is related to the estimate of the number of background muonless events from hadronic showers.

Hadronic interaction models. The largest uncertainty comes from the variety of models of shower development that predict different values of the muon number in EASs. Furthermore, this difference is sensitive to the muon threshold energy, which is 10 GeV in our case. The change of the expected muon density in an EAS by ±10 % would result in the change of the number of background muonless showers in the sample by ±4. The results we quote are based on the QGSJET-01 model [29], which gives a good description of the LHC and Pierre Auger Observatory measurements of the high-energy hadronic cross section (cf. Fig. 5 in Ref. [21]) and of the LHC multiplicity distributions (see, e. g., Ref. [32]); the choice of the model was also motivated by its computational efficiency. The amount of model-to-model variations of the number of > 10 GeV muons in EASs can be estimated from Ref. [33] and from our own simulations. The effect of the change of the interaction model on our results is summarized in Table 2. We note that according to experimental data on EAS development, all hadronic-interaction models currently in use significantly underestimate the number of muons in a shower. In particular, several independent indirect analyses of the Pierre Auger Observatory data indicate [37] that the real number of muons is approximately 1.5 times larger than predicted by the QGSJET II-03 model. This number is used in Table 2 and for the estimate of the systematic error; a similar result was obtained with the help of muon detectors of the Yakutsk EAS array [38, 39]. The systematic error in the resulting gamma-ray flux due to the uncertainty of hadronic models is ±50 %, with the upper value favored by the experimental data.

Primary composition. The assumption of a purely proton composition gives a conservative (i. e., large) estimate of the expected background of the muonless events because primary heavier nuclei produce more muons in EASs. For primary iron, the corresponding number of muons is larger by a factor of ~ 2.5, which shifts the expected background downward to zero. This would change our fraction and flux estimates by +90 %.

Large fluctuations. Because no model gives a perfect description of hadron-induced air showers, and in particular there are large uncertainties in predictions of the muon number, we cannot exclude that the fluctuations of the EAS muon content might be much larger than suggested by simulations. Among theoretical approaches, the probability of an occasional very low muon density in a proton shower is the highest in the model in Ref. [40], where the energy equipartition between positive, negative, and neutral components of the cascade was postulated. As has been shown in Ref. [41], in the framework of this model, it is possible to obtain the probability of ~ 1 % of imitation of a gamma-ray shower by a primary proton. However, this model is much less physically motivated compared to those that are currently used in simulation codes.

Table 2. Effect of the choice of hadronic interaction models on the result. The last line corresponds to experimental results on the muon content of EASs

Model	$\frac{N_\mu}{N_\mu(\text{QGSJET-01})}$	Expected number of muonless events	Excess number of muonless events
SIBYLL 2.1 [34]	0.70	38.0	10.7
QGSJET II-03 [35]	0.89	27.6	21.0
QGSJET-01 [29]	1.00	23.5	25.2
EPOS 1.99 [36]	1.03	21.9	26.8
Experiment [37]	1.33	10.9	37.8

To summarize the discussion of systematic uncertainties, current experimental and theoretical understanding of the EAS properties suggests that the flux values we obtain are conservative, although they could become lower if physically less motivated models were used for hadronic showers.

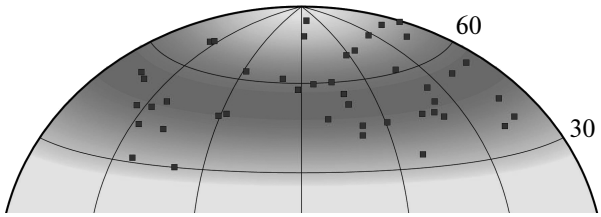

Fig. 5. The distribution of arrival directions of muonless events in the sky (equatorial coordinates). Grayscale represents the distribution expected for the isotropic flux

4. ARRIVAL DIRECTIONS

In this section, in order to find some hints about the origin of the events we observed, we perform various searches for deviations from isotropy in the distribution of the arrival directions of photon-like events. All the tests are performed by comparison, by means of a certain statistical procedure, of the real distribution of arrival directions with a simulated one, which assumes isotropy. In all cases, the result of a test is given by the probability P that the actual distribution of events is a fluctuation of the isotropic distribution, that is, for small P, the isotropic distribution is excluded at the confidence level of $1 - P$. For tests of the global (large-scale) isotropy, we use the Kolmogorov–Smirnov method (see, e. g., Ref. [42]), which compares one-dimensional distributions of real and simulated events in some observable (e. g., a celestial coordinate). For searches of the local (small-scale) anisotropy, we rely on the correlation-function method, which estimates how often the number of pair coincidences of directions from two catalogs (e. g., one of the arrival directions of cosmic rays and another of particular astronomical objects) in simulated samples exceeds the similar number obtained from the real data. The notion of the "pair coincidence" depends on the angular distance Δ between the directions, and hence the probability $P(\Delta)$ is often quoted for a certain range of Δ. The clustering properties of the sample of the directions are estimated by the same method with both catalogs being identical cosmic-ray lists. More details on the method can be found, e. g., in Ref. [43].

In both approaches, we need to simulate sets of arrival directions under the assumption of an isotropic flux. These sets should take the experimental selection effects into account. For continuously operating surface detector arrays with the efficiency close to 100 %, the exposure is uniform in the azimuth angle and depends on the zenith angle θ via a purely geometric factor $\sin\theta\cos\theta$, assuming that the incoming flux is isotropic (this is the case if an energy-limited sample of cosmic rays is studied). However, our sample is limited by N_e instead of energy and, due to different ages of showers coming at different zenith angles, the exposure becomes nongeometric. Based on the observed distribution of θ, we determine the acceptance factor as $\sim \sin\theta\cos^9\theta$. The distribution of events in the azimuth angle is perfectly consistent with a uniform distribution, as expected. The distribution of the arrival directions on the sky, together with the one expected from exposure for the isotropic flux, is shown in Fig. 5. In the study of the arrival directions, we do not include 3 of 48 events observed in 1982 for which the determination of geometry is uncertain.

4.1. Possible scenarios for UHE photons

Among possible mechanisms of the origin of UHE gamma rays, we separately consider those that do not require deviations from the standard particle-physics and astrophysical concepts (we call these scenarios conventional) and those that require the presence of particles and/or interactions beyond the Standard Model of particle physics (these are called "new-physics" scenarios). We note that high-energy photons interact with cosmic background radiation efficiently. Assuming the standard physics, the energy attenuation length for a $\sim 10^{17}$ eV photon is as low as ~ 35 kpc due to the efficient e^+e^- pair production on the cosmic microwave background (CMB). This means that the observed photons were created in the Galaxy unless some new physics is assumed.

4.1.1. Conventional scenarios

Scenario 1. Cosmogenic photons. UHE cosmic particles experience intense interactions with cosmic background radiation. For protons with energies above $\sim 5 \cdot 10^{19}$ eV, these are dominated by the GZK [44, 45] process of pion production through the Δ resonance; for lower energies, the dominant mechanism is the e^+e^- pair production. For heavier primaries at $E \sim 10^{20}$ eV, photodisintegration effectively reduces the propagation effects to those of protons of lower energy. The secondary particles from all these interactions (pions, electrons, and positrons) are the source of the so-called cosmogenic photons, which appear either from subsequent pion decays or from inverse Compton scattering of $e^{\pm}$. There are numerous works on the GZK photons (see, e. g., Refs. [46, 47]); the key point of interest here is the possibility to use these $\sim (10^{18}$–$10^{19})$ eV gamma-rays as a tool to determine the composition of the bulk of $E \sim 10^{20}$ eV cosmic rays; due to the GZK process, the flux of the secondary photons would be much higher for super-GZK protons than for heavy nuclei. Given the present-day uncertainty in the primary composition at the very end of the CR spectrum (see, e. g., Refs. [20, 21]), this approach attracts considerable attention, although no sign of the GZK photons have yet been observed. The expected flux of GZK photons at $E \lesssim 10^{17}$ eV is far too low to explain our result; we are not aware of a calculation of the flux at lower energies, nor of the distribution of their arrival directions (which should be close to the isotropic one, however).

Scenario 2. Direct photons from point-like sources. UHE astrophysical accelerators are expected to emit energetic photons born in interactions of charged particles with ambient matter and radiation. The energy of accelerated particles should therefore exceed the energy of the photons, roughly by an order of magnitude. It is presently unknown whether the acceleration of particles up to $\sim (10^{17}$–$10^{18})$ eV can occur in any single object in the Galaxy (that is, within the propagation length of $\sim 10^{17}$ eV photons). In any case, these objects are not expected to be numerous; we therefore expect a certain degree of clustering of the arrival directions of photons in this scenario. Galactic TeV gamma-ray sources may represent plausible candidates for the UHECR accelerators; in this case, the arrival directions would concentrate around them.

4.1.2. "New-physics" scenarios

Scenario 3. Superheavy dark matter. While the Large Hadron Collider failed to easily discover any dark-matter candidate, models of dark matter that are beyond the reach of this machine are becoming more and more popular. In particular, the superheavy dark matter (SHDM) scenario (mass $M \gtrsim 10^{18}$ eV), originally put forward in [48] to explain the apparent excess of $E \gtrsim 10^{20}$ eV cosmic rays (presently disfavored), has its own cosmological motivation. Its important prediction is a significant fraction of secondary photons among the decay products of these superheavy particles; these energetic photons contribute to the UHECR flux. For $M \gtrsim 10^{20}$ eV, the scenario is constrained, but not killed [49], by the UHE photon limits; constraints for lower M have not been studied. A characteristic manifestation of this mechanism is a Galactic anisotropy [50] of the arrival directions of photons related to the noncentral position of the Sun in the Galaxy.

Scenario 4. Axion-like particles and BL Lac correlations. The UHECR data set with the best angular resolution ever achieved (0.6°), that of High Resolution Fly's Eye (HiRes) in the stereo mode, demonstrated hard-to-explain correlations of arrival directions of $E \gtrsim 10^{19}$ eV events with distant astrophysical sources, BL Lac type objects [51, 52], which suggest that $\sim 2\,\%$ of the CR flux at these energies is neutral particles arriving from these objects. The only self-consistent explanation of this phenomenon [24] not requiring violation of the Lorentz invariance suggests that the observed events are caused by gamma-rays that mix with hypothetical new light particles (axion-like particles, ALPs) in cosmic magnetic fields. This would allow them to propagate freely through the cosmic photon background in the form of the inert ALP and then to

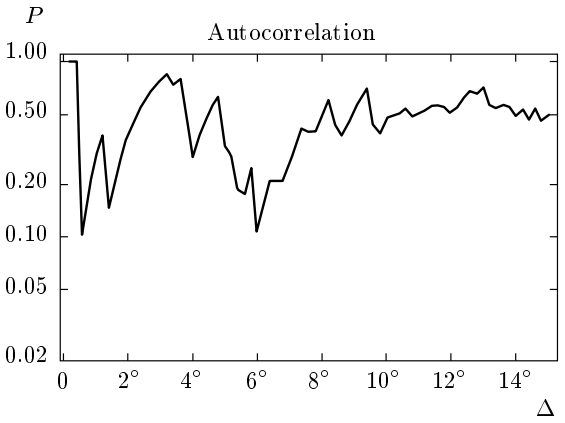

Fig. 6. The autocorrelation test: the probability $P(\Delta)$ to have the observed or higher number of pairs of events within the angular bin Δ as a fluctuation of the isotropic distribution

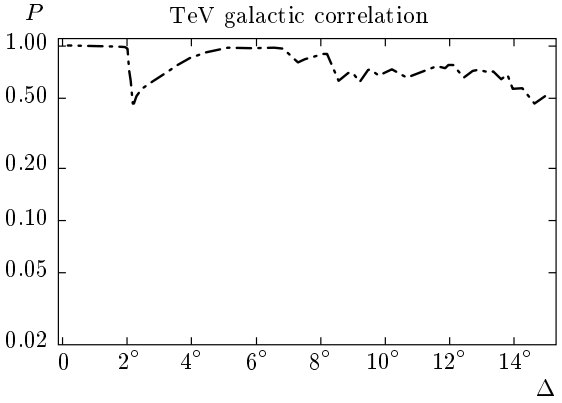

Fig. 7. The test of correlation with Galactic TeV sources: the probability $P(\Delta)$ to have the observed or higher number of events within the angular distance Δ from TeVCat [53] Galactic TeV sources as a fluctuation of the isotropic distribution

convert back to real photons in a region of the magnetic field close to the observer. This approach may also explain some other astrophysical puzzles. A test of this scenario may be performed by cross-correlation of the arrival directions with the same BL Lac catalog as in Refs. [51, 52].

Scenario 5. Lorentz-invariance violation. There is no lack of theoretical models with tiny violation of the relativistic invariance on the market. In some of them, this effect results in an efficient increase of the mean free path of an energetic photon through CMB [23]. Although these models have many free parameters, with no particularly motivated choice, one may expect that a possible effect of this change of the attenuation length would be to increase the cosmogenic-photon flux at $E \lesssim 10^{17}$ eV by orders of magnitude. There is no evident signature of this scenario in arrival directions.

4.2. Distribution of arrival directions of muonless events

4.2.1. Point-like or diffuse sources?

The test of the presence of a relatively small number of point-like sources is provided by the autocorrelation function. We present the results in Fig. 6, where the probability that the observed excess of pairs of events is in the angular bin Δ is plotted as a function of Δ. No significant clustering of events is found.

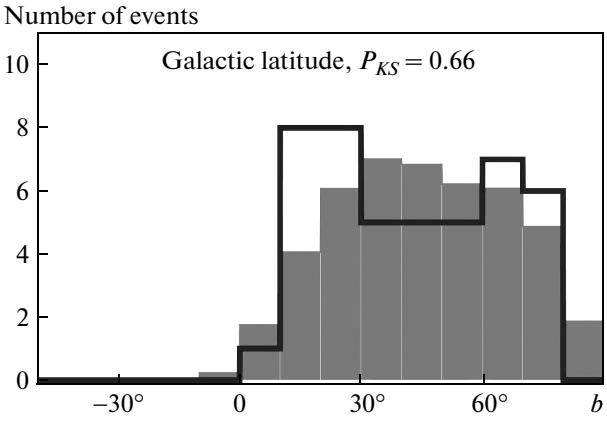

Fig. 8. The distribution of the observed photon-like events (line) and Monte Carlo isotropic events (gray) as a function of the Galactic latitude b

4.2.2. Test of scenario 2: Galactic TeV sources

Figure 7 represents the $P(\Delta)$ function for cross-correlations of the arrival directions of the photon-like events with positions of Galactic TeV sources from the TeVCat catalog [53], as of May 2013. No sign of correlation is seen.

4.2.3. Test of scenario 2: Galactic-plane correlation

Galactic UHECR accelerators of a yet unknown type are still expected to concentrate along the Galactic plane, and the distribution of events in the Galactic latitude b is a model-independent test of this scenario. Figure 8 illustrates that the distribution of photon-

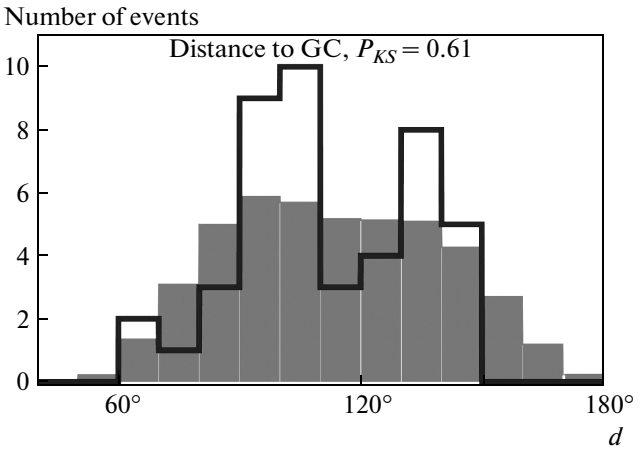

Fig. 9. The distribution of the observed photon-like events (line) and Monte Carlo isotropic events (shadow) as a function of the angular distance to the Galactic Center

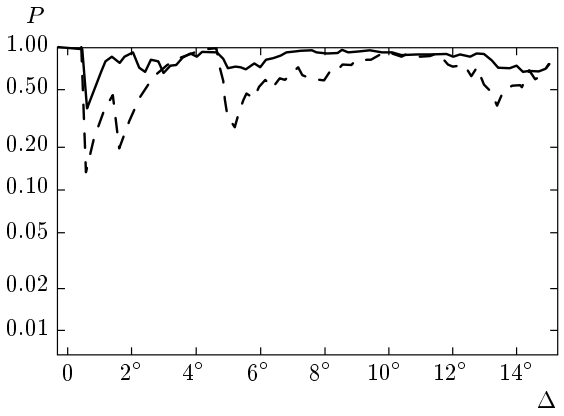

Fig. 10. The test of correlation with BL Lac type objects: the probability $P(\Delta)$ to have the observed or higher number of events within the angular distance Δ from bright Vèron BL Lacs (sample of Ref. [51], solid line) and TeVCat [53] TeV BL Lacs (dashed line) as a fluctuation of the isotropic distribution

like events over b is consistent with that expected for an isotropic flux (the Kolmogorov–Smirnov probability $P_{\rm KS} \approx 0.66$).

4.2.4. Test of scenario 3: Galactic anisotropy

The SHDM-related Galactic anisotropy should reveal itself in the dipole excess seen in the distribution of events as a function of the distance to the Galactic Center. Figure 9 demonstrates that no such excess is seen ($P_{\rm KS} \approx 0.61$).

4.2.5. Test of scenario 4: BL Lac correlations

The HiRes BL Lac correlations [51] appeared as an excess of events close to positions of 156 bright BL Lac type objects selected from the catalog [54] by the cut on the optical magnitude $V < 18^{\rm m}$. A subsequent study [52] also suggested a correlation with TeV-selected BL Lacs. In Fig. 10, we present the results of a similar analysis for our photon-like sample, with the same catalog of 156 BL Lacs and with an updated list of TeV BL Lacs from TeVCat [53]. No significant correlation is seen.

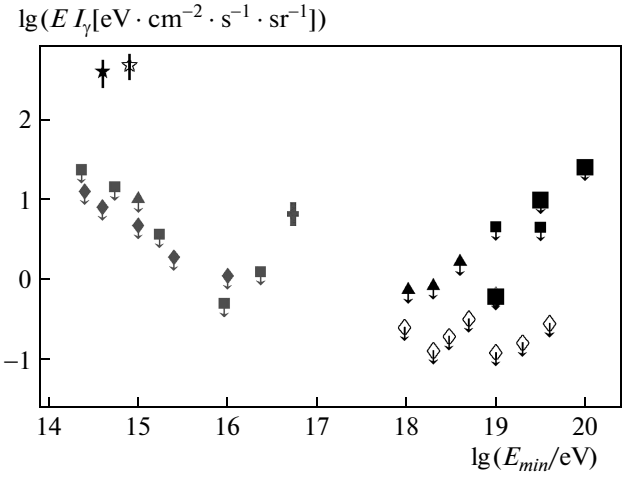

Fig. 11. The diffuse cosmic photon integral flux versus the photon minimal energy. The result of this paper is shown as a cross whose vertical line represents the error bars. Tentative detections and upper limits from other experiments are indicated by symbols: star (Tien Shan [17], detection), open star (Lodz [19], detection), gray triangle (EAS-TOP [4]), gray squares (CASA-MIA [5]), gray diamonds (KASCADE [6, 55]), triangles (Yakutsk [12]), open diamonds (Pierre Auger [13, 14]), boxes (AGASA [8]), and large squares (Telescope Array [15])

5. DISCUSSION AND CONCLUSIONS

The place of our result among others is rather specific. All previous studies put upper limits on the photon flux or fraction for the primary energy intervals $\sim (10^{14}$–$5 \cdot 10^{16})$ eV and $\gtrsim 10^{18}$ eV. The EAS-MSU result, first reported in Ref. [26], therefore represents the first ever statistically significant detection of cosmic photons with energies above ~ 100 TeV. In this paper,

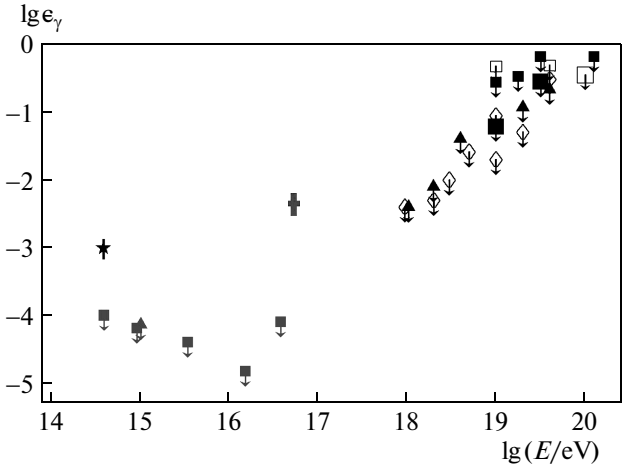

Fig. 12. The fraction of gamma-ray primaries in the diffuse cosmic-ray integral flux versus the photon minimal energy. The notation is the same as in Fig. 11; in addition, more Yakutsk results [11], results from Haverah Park ([7], open squares), from reanalysis of the AGASA data ([9], the highest-energy square like AGASA), and from a combination of AGASA and Yakutsk data ([10], large open square) are shown

we performed the first estimate of the gamma-ray flux in the previously unstudied energy window $(5 \cdot 10^{16}$–$10^{18})$ eV and estimated statistical and systematic errors for its value. The result is compared with limits obtained by other experiments in Fig. 11 (flux) and Fig. 12 (fraction). The fraction estimates should be interpreted with great care because they are sensitive to the energy determination of the bulk of hadronic primaries, which is known to suffer from large systematic uncertainties due to the lack of understanding of high-energy hadronic interactions. By contrast, the photon flux estimates are more robust because they use the primary gamma-ray energy determination and the exposure of the array only, both quantities being well understood. Therefore, the main result in this paper is the flux estimate in Eq. (1).

The interpretation of the result is problematic. Leaving aside the discrepancy with the CASA-MIA result in terms of the (uncertain) gamma-ray fraction, the more robust flux estimate, Eq. (1), does not formally contradict any existing experimental constraint, but is clearly in conflict with the general trend observed at both lower and higher energies[1)], see Fig. 11. Within the conventional scenarios, these photons cannot travel longer than a few dozen Mpc and should therefore be born in the Galaxy. However, we do not see any significant Galactic (nor any other) anisotropy in the distribution of the arrival directions. To add to the troubles, in some scenarios it would be difficult to avoid a conflict with measurements of the ~ 1 GeV diffuse photon flux to which secondary photons from electromagnetic cascades in the Universe have to contribute.

The estimates we made were obtained under the assumption that the muonless events that are not accounted for by fluctuations of hadronic showers, and only these events, are caused by primary photons. This assumption is a reasonable first approximation, but it suggests two directions for future work. First, gamma-ray showers have a small but nonzero number of muons (the reason for the appearence of muons is in the photonuclear interactions). The presence of a certain number of muonless events implies, within the photon hypothesis, that there should be an excess of muon-poor events in the data, which is yet to be tested. Second, there are other observables, not directly related to the muon number, which may distinguish photon showers from hadronic ones. One approach is to study the shower front curvature, which is related to the depth of the maximal development of the electromagnetic cascade; it has been used to search for primary photons in the experiments that do not have muon detectors (see, e. g. [15]). This method is particularly prospective for the EAS-MSU data because the array was dense and the number of detector stations that recorded a $N_e \gtrsim 10^7$ shower was typically large.

The result we present may be tested with the muon data of the Yakutsk EAS array and in future experiments like fluorescence detectors of the Telescope-Array low-energy extension (TALE) [56], muon detectors of the Pierre Auger Observatory infill array (AMIGA) [57], or Cerenkov and muon detectors of the Tunka-HiSCORE [58].

The study of arrival directions of muonless events did not reveal any significant deviation from isotropy that might give a clue to their origin. In principle, this may change with the extension of the data set to an energy-limited sample (versus N_e limited one), which would increase the statistics for inclined events, together with more precise determination of the arrival directions and reduction of the background by means of two-parameter (e. g., both the muon number and shower-front curvature) selection of photon-like showers. We leave these questions for a future study.

We are indebted to O. Kalashev and G. Rubtsov for the helpful discussions. The work of N. K., G. K.,

[1)] We note in passing that Eq. (1) agrees well with the early Yakutsk estimate [18] of the $\sim 10^{17}$ eV photon flux, but that claim was based on the observation of one event only.

V. S., and Yu. F. was supported in part by the RFBR (grant № 11-02-00544) and by the Ministry of Science and Education of the Russian Federation (agreement № 14.518.11.7046). The work of S. T. was supported in part by the RFBR (grants №№ 11-02-01528, 12-02-01203, 13-02-01311, 13-02-01293) and by the Ministry of Science and Education of the Russian Federation (agreements №№ 8142 and 14.B37.21.0457).

REFERENCES

1. G. B. Khristiansen, G. V. Kulikov, and Yu. A. Fomin, *Ultra-High-Energy Cosmic Radiation*, Atomizdat, Moscow (1975).
2. M. Risse and P. Homola, Mod. Phys. Lett. A **22**, 749 (2007) [arXiv:astro-ph/0702632].
3. T. Tanimori, K. Sakurazawa, S. A. Dazeley et al. [CANGAROO Collaboration], Astrophys. J. **492**, L33 (1998) [arXiv:astro-ph/9710272].
4. M. Aglietta, B. Alessandro, P. Antoni et al. [EAS-TOP Collaboration], Astropart. Phys. **6**, 71 (1996).
5. M. C. Chantell, C. E. Covault, J. W. Cronin et al. [CASA-MIA Collaboration], Phys. Rev. Lett. **79**, 1805 (1997) [arXiv:astro-ph/9705246].
6. G. Schatz, F. Fessler, T. Antoni et al. [KASCADE collaboration], *Proc. 28th ICRC*, Tsukuba, **1**, 2293 (2003).
7. M. Ave, J. A. Hinton, R. A. Vazquez et al., Phys. Rev. Lett. **85**, 2244 (2000) [arXiv:astro-ph/0007386].
8. K. Shinozaki, M. Chikawa, M. Fukushima et al. [AGASA Collaboration], Astrophys. J. **571**, L117 (2002).
9. M. Risse, P. Homola, R. Engel et al., Phys. Rev. Lett. **95**, 171102 (2005) [arXiv:astro-ph/0502418].
10. G. I. Rubtsov, L. G. Dedenko, G. F. Fedorova et al., Phys. Rev. D **73**, 063009 (2006) [arXiv:astro-ph/0601449].
11. A. V. Glushkov, D. S. Gorbunov, I. T. Makarov et al., JETP Lett. **85**, 131 (2007) [arXiv:astro-ph/0701245].
12. A. V. Glushkov, I. T. Makarov, M. I. Pravdin et al., Phys. Rev. D **82**, 041101 (2010) [arXiv:0907.0374 [astro-ph.HE]].
13. J. Abraham, P. Abreu, M. Aglietta et al. [Pierre Auger Collaboration], Astropart. Phys. **29**, 243 (2008) [arXiv:0712.1147 [astro-ph]].
14. P. Abreu, M. Aglietta, E. J. Ahn et al. [Pierre Auger Collaboration], arXiv:1107.4805 [astro-ph.HE].
15. T. Abu-Zayyad, R. Aida, M. Allen et al. [Telescope Array Collaboration], arXiv:1304.5614 [astro-ph.HE].
16. K. Suga, Y. Toyoda, K. Kamata et al., Astrophys. J. **326**, 1036 (1988).
17. S. I. Nikolsky, I. N. Stamenov, and S. Z. Ushev, J. Phys. G **13**, 883 (1987).
18. A. V. Glushkov, N. N. Efimov, N. N. Efremov et al., *Proc. 19th ICRC*, La Jolla, **2**, 186 (1985).
19. J. Gawin, R. Maze, J. Wdowczyk, and A. Zawadzki, Canad. J. Phys. **46**, 75 (1968).
20. K.-H. Kampert and M. Unger, Astropart. Phys. **35**, 660 (2012) [arXiv:1201.0018 [astro-ph.HE]].
21. S. Troitsky, Phys. Usp. **56**(3), (2013), Uspekhi Fiz. Nauk **183**, 323 (2013) [arXiv:1301.2118 [astro-ph.HE]].
22. P. Bhattacharjee and G. Sigl, Phys. Rept. **327**, 109 (2000) [arXiv:astro-ph/9811011].
23. M. Galaverni and G. Sigl, Phys. Rev. Lett. **100**, 021102 (2008) [arXiv:0708.1737 [astro-ph]].
24. M. Fairbairn, T. Rashba and S. V. Troitsky, Phys. Rev. D **84**, 125019 (2011) [arXiv:0901.4085 [astro-ph.HE]].
25. S. N. Vernov, G. B. Khristiansen, V. B. Atrashkevich et al., Bull. Russ. Acad. Sci. Phys. **44**, 80 (1980) [Izv. Ross. Akad. Nauk Ser. Fiz. **44**, 537 (1980)].
26. N. Kalmykov, J. Cotzomi, V. Sulakov et al., Izv. Ross. Akad. Nauk Ser. Fiz. **75**, 584 (2009).
27. Yu. A. Fomin, N. N. Kalmykov, V. M. Kalmykov et al., *Proc. 28th ICRC*, Tsukuba, **1**, 119 (2003).
28. S. J. Sciutto, *AIRES: A System for Air Shower Simulations. Version 2.6.0* (2002).
29. N. N. Kalmykov, S. S. Ostapchenko, and A. I. Pavlov, Nucl. Phys. Proc. Suppl. B **52**, 17 (1997).
30. A. A. Lagutin, V. V. Uchaikin, and G. V. Chernyaev, Yad. Fiz. **45**, 757 (1987).
31. N. N. Kalmykov, L. A. Kuzmichev, G. V. Kulikov et al., Moscow Univ. Phys. Bull. **65**, 275 (2010).
32. D. d'Enterria, R. Engel, T. Pierog et al., Astropart. Phys. **35**, 98 (2011) [arXiv:1101.5596 [astro-ph.HE]].
33. R. Engel, *Talk at the International Symposium on Future Directions in UHECR Physics*, CERN, 13–16 February 2012.
34. E.-J. Ahn, R. Engel, T. K. Gaisser et al., Phys. Rev. D **80**, 094003 (2009) [arXiv:0906.4113 [hep-ph]].

35. S. Ostapchenko, Nucl. Phys. Proc. Suppl. **151**, 143 (2006) [arXiv:hep-ph/0412332].

36. T. Pierog and K. Werner, Nucl. Phys. Proc. Suppl. **196**, 102 (2009) [arXiv:0905.1198 [hep-ph]].

37. R. Engel [Pierre Auger Collaboration], arXiv: 0706.1921 [astro-ph].

38. A. V. Glushkov, I. T. Makarov, M. I. Pravdin et al., JETP Lett. **87**, 190 (2008) [arXiv:0710.5508 [astro-ph]].

39. L. G. Dedenko, G. F. Fedorova, T. M. Roganova et al., J. Phys. G **39**, 095202 (2012).

40. V. V. Uchaikin and V. V. Ryzhov, *The Stochastic Theory of High Energy Particle Transport*, Nauka, Novosibirsk, Siberian Branch (1988) (in Russian).

41. J. Cotzomi Paleta, *PhD Thesis, SINP MSU*, Moscow (2010).

42. W. H. Press, S. A. Teukolsky, W. T. Vetterling, and B. P. Flannery, *Numerical Recipes: The Art of Scientific Computing*, Cambridge University Press, Cambridge (2007).

43. P. Tinyakov and I. Tkachev, Phys. Rev. D **69**, 128301 (2004) [arXiv:astro-ph/0301336].

44. K. Greisen, Phys. Rev. Lett. **16**, 748 (1966).

45. G. T. Zatsepin and V. A. Kuzmin, JETP Lett. **4**, 78 (1966) [Pisma Zh. Eksp. Teor. Fiz. **4**, 114 (1966)].

46. G. Gelmini, O. E. Kalashev, and D. V. Semikoz, J. Exp. Theor. Phys. **106**, 1061 (2008) [arXiv: astro-ph/0506128].

47. D. Hooper, A. M. Taylor, and S. Sarkar, Astropart. Phys. **34**, 340 (2011) [arXiv: 1007.1306 [astro-ph.HE]].

48. V. Berezinsky, M. Kachelriess, and A. Vilenkin, Phys. Rev. Lett. **79**, 4302 (1997) [arXiv:astro-ph/9708217].

49. O. E. Kalashev, G. I. Rubtsov, and S. V. Troitsky, Phys. Rev. D **80**, 103006 (2009) [arXiv:0812.1020 [astro-ph]].

50. S. L. Dubovsky, P. G. Tinyakov, and I. I. Tkachev, Phys. Rev. Lett. **85**, 1154 (2000) [arXiv: astro-ph/0001317].

51. D. S. Gorbunov, P. G. Tinyakov, I. I. Tkachev, and S. V. Troitsky, JETP Lett. **80**, 145 (2004) [Pisma Zh. Eksp. Teor. Fiz. **80**, 167 (2004)] [arXiv: astro-ph/0406654].

52. R. U. Abbasi et al. [HiRes Collaboration], Astrophys. J. **636**, 680 (2006) [arXiv:astro-ph/0507120].

53. TeVCat, `http://tevcat.uchicago.edu/`.

54. M. P. Véron-Cetty and P. Véron, Astron. Astrophys. **374**, 92 (2001).

55. M. Risse and G. Rubtsov, *Talk at the International Symposium on Future Directions in UHECR Physics*, CERN, 13–16 February 2012.

56. S. Ogio et al. [Telescope Array Collaboration], *Talk at the International Symposium on Future Directions in UHECR Physics*, CERN, 13–16 February 2012.

57. A. Etchegoyen [Pierre Auger Collaboration], arXiv: 0710.1646 [astro-ph].

58. M. Tluczykont, D. Hampf, U. Einhaus et al., AIP Conf. Proc. **1505**, 821 (2012).